Proceedings of IMECE2008
2008 ASME International Mechanical Engineering Congress and Exposition
October 31- November 6, 2008, Boston, Massachusetts, USA

IMECE2008-66946

FABRICATION, CHARACTERIZATION AND MICROSENSING OF WHISPERING-GALLERY MODE MICRO-COUPLING SYSTEMS

Qiulin Ma
Department of Mechanical and Aerospace Engineering, Rutgers University
Piscataway, NJ 08854, USA

Tobias Rossmann
Department of Mechanical and Aerospace Engineering, Rutgers University
Piscataway, NJ 08854, USA

Zhixiong Guo
Department of Mechanical and Aerospace Engineering, Rutgers University
Piscataway, NJ 08854, USA

ABSTRACT

An optical micro-coupling system of whispering-gallery mode usually consists of a resonator (e.g. a sphere) and a coupler (e.g. a taper). In this report, silica microspheres of 50–500μm in diameter are fabricated by hydrogen flame fusing of an end of a single mode fiber or fiber taper. Fiber tapers are fabricated by the method of heating and pulling that meets an adiabatic condition. Taper's waist diameter can routinely be made less than 1μm and almost zero transmission loss in a taper is achieved which allows an effective and phase-matched coupling for a wide range sizes of microspheres. Both resonators and couplers' surface microstructure and shapes are examined by scanning electronic microscopy. Three regimes of coupling are achieved, enabling a good flexibility to control *Q* value and coupling efficiency of a micro-coupling system. Whispering gallery mode shift is used to demonstrate a novel temperature micro-sensor. Its sensitivity determined from actual experimental results agrees well with the theoretical value. A concept of using the photon's cavity ring down (CRD) in the microsphere to make a novel high-sensitivity trace gas micro-sensor is proposed. The CRD time constant when ammonia is chosen as the analyte gas is predicted using the simulated absorption lines.

1. INTRODUCTION

Whispering-gallery mode (WGM) effects in dielectric microresonators have been extensively studied over the past several years due to their distinct feature of very high quality factor (Q) in small mode volume which attracts growing interest in experimental cavity quantum electrodynamics[1], laser frequency stabilization[2], microlasers[3~6], and sensor applications[7,8]. The WGM's propagate on a circular path around the micro-resonator which can be a disk, a ring, or a sphere, remaining confined in a thin layer beneath the surface. They correspond to electromagnetic waves trapped and resonated in circling orbits just within the surface of the cavity, being continuously totally reflected from the surface. Under these circumstances, the leakage of the light can be extremely low and thus gives very high *Q* values[9]. The spherical WGM's are by convention characterized in terms of three mode numbers representing the radial, azimuthal, and polar fields distributions. The radial part can be described by spherical Bessel functions, the polar field follows spherical harmonics, and the azimuthal field varies sinusoidally [10,11]. For practical purposes, we are usually interested in exciting modes that are mostly confined to the surface of the sphere and to the sphere equator, which are the ones with lowest mode volume [12].

The modes in a WGM microcavity are highly confined and thus are not accessible by free-space beam. Therefore, to couple the light in and out of the cavity is another crucial point. Employments of near-filed couplers are required. An evanescent field generated at a surface which totally reflected light in the other side was shown to be the most promising approach to transfer power from the coupler into the whispering gallery modes. A prism can be used to efficiently couple the light into and out of the microsphere [13], however, it requires bulky component and it works with awkward alignment. A fiber half-block consisting of an polished fiber buried in glass exposes the core and thus allows access to the

optical mode[11], but it has leakage of light from the sphere modes into the fiber cladding and the half-block and thus spoils *Q* value and coupling efficiency. A fiber-prism or angle polished fiber is efficient in coupling and combines the advantage of waveguide light insertion with prism coupling but eliminates most of the alignment steps for bulky prism couplers [14]. However, it requires delicate cutting and polishing the end of the fiber tip. What we focus on in this paper is tapered fiber coupler which is a very powerful coupling tool. It allows sensitive tuning of the fiber mode propagation constant by controlling the size of the fiber thickness or scanning the microsphere across different size part region of the taper. It can not only align with the microsphere easily but also efficiently couple the light into and out of the microsphere cavities [12].

In this paper, we fabricated taper by heating and pulling a single mode fiber. The transmission signals during the taper fabrication are recorded and demonstrate that we can fabricate fiber taper with almost no tapering loss while having a sub-micron waist size confirmed by SEM measurement. We applied the phase-matched coupling to get an idea of matching the sizes of the fiber taper and microsphere, and demonstrate it in experiment with WGM spectrum. Furthermore, a more delicate coupling is achieved to leave an air gap between the microsphere and fiber taper and thus demonstrate a three regimes of coupling, overcoupling, critical coupling and undercoupling. The *Q* value and coupling efficiency can be well controlled by these coupling regimes.

For sensor application, the WGM micro-coupling system can be applied to trace the analyte around the microsphere by *Q*-spoiling due to absorption, as well as to sense the properties of the surrounding medium by monitoring the WGM resonance frequency shift due to a change of refractive index or of the effective size of the microsphere. In this paper, we experimentally demonstrate a novel temperature sensor by monitoring the WGM resonance frequency shift and its sensitivity is very close to the theoretical value. Another sensor based on the scheme of cavity ring down spectroscopy is proposed. The life time of a photon trapped in WGM mode will decrease when surrounding medium absorbs the power of the evanescent wave. Ammonia is chosen as the analyte since its absorption lines are strong and condensed in the telecommunication band we use for WGM. A theoretical prediction of the cavity ring down time change due to absorption is made to demonstrate that a high sensitivity sensor is promising.

2. FABRICATION OF MICROSPHERE

The material we used for microsphere fabrication is Corning SMF-28 silica fiber. It is a standard telecommunication single mode fiber with core diameter about 8.2μm and cladding diameter about 125μm. The core is slightly doped silica with slightly higher index of refraction than the cladding which is made of pure silica. Fig.1 is an SEM image we took for the crossection of a stripped and cleaved fiber. Only core and cladding are remained, and can be clearly distinguished in the image. Core only takes a small portion in this silica rod which is good to fabricate microspheres with uniform component distribution. In the ultraviolet regime metallic impurities degrade the transmittance while in the infrared water is the principal impurity of attenuation. Years of efforts in fiber optic communication has led to industrial production of very high quality (<5ppm –OH) SMF-28 fiber which has a very low attenuation of $\leqslant$ 0.22dB/km for telecommunication band 1525-1575*nm*.

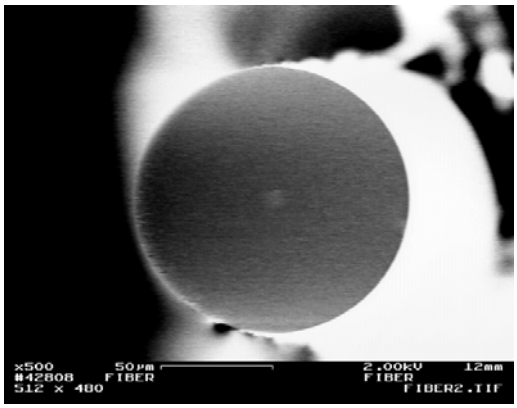

Fig.1 SEM image of the cross-section of a stripped Corning SMF-28 fiber.

The high-*Q* microspheres are fabricated from extremely clean and smooth stripped and cleaved fiber. A stripped fiber should be exposed in air as short as possible before completing the fabrication, since silica absorbs atmospheric water vapor and gets contaminated. In addition, dirt, grease and dust collect on the surface must also be removed. Kimwipes delicate task wipers are used to scrub the stripped fiber with a glassware detergent Alconox and volatile solvent Enthanol to initially clean the fiber. Then the stripped fibers are put into Enthanol again and cleaned in ultrasonic cleaner (Fisher Scientific) to detach any residues on the fiber. The final step for fiber preparation is to spray the fiber with ultra pure duster right after getting it out of the ultrasonic cleaning solvent. The fiber is then used right away for fiber fabrication.

The silica microspheres are fabricated by melting the tip of an appropriately prepared fiber. The melting of the silica can be performed by CO_2 laser[4], electric arc[15] or oxy-hydrogen flame heating[9]. All these techniques have been found to produce a minimal amount of soot that can spoil the quality of the sphere. We choose to use an oxy-hydrogen micro-torch. The flame temperature can be easily controlled by adjusting the combustion ratio of oxygen and hydrogen, varying from about 2400K (hydrogen in air) to about 3080K (stoichiometric mixture of oxygen and hydrogen)[16]. And the power can be controlled by varying the gas flow rates. During the fabrication, once the silica passes the melting point, surface tension shapes the material into a spheroidal form. At this point, the sphere glows hot white and it is then moved slowly out to lower temperature part of the flame to do seconds of annealing.

Annealing reduces the density variation and allows time for small surface variations being smoothed out by surface tension. And it solidifies immediately after fully getting out the flame. The fused spheres have a size about 50-500μm, depending on the size of stripped fiber. For example, by carefully melting a very thin taper of about several microns in appropriate part of the flame, smaller spheres can be obtained. Fig.2 shows an SEM image of two microspheres fabricated from untapered and tapered fiber. Fig.3 shows the surface microstructure of the small microsphere in Fig.2, which is also typical for other sizes of microspheres. Only nano-scale dips and bumps appear on the surface which proves the smoothness of the spheres.

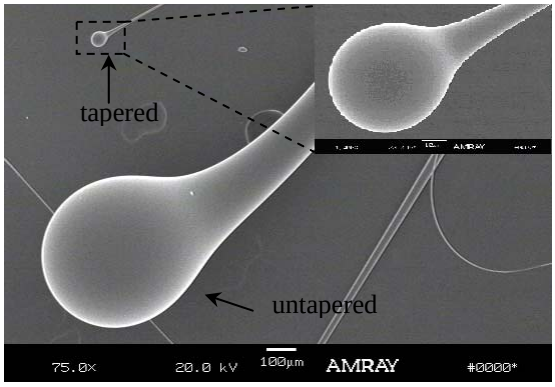

Fig.2 SEM image of two microspheres fabricated from untapped and taped fiber, respectively.

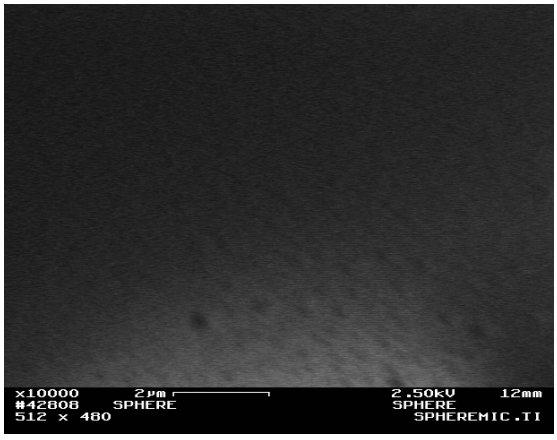

Fig.3 SEM image of the surface of the small mircrosphere.

3. FABRICATION OF FIBER TAPER

In the untapered single mode fiber SMF-28, light is guided and confined in the core. The evanescent wave is not exposed for near-filed coupling. A fiber taper is thus needed for accessing the evanescent wave. Two ways of fabrication have been tried, chemical etching and pulling. Hydrofluoric acid is used to perform etching, which essentially etches away the cladding so that the air becomes cladding and evanescent wave is exposed. However, in order to get a smooth taper, it takes hours to use low concentration acid for etching. Cleaning the acid residue left on the taper after fabrication is also inevitable for getting smooth and undegraded taper. In addition, it is very difficult to get a very thin taper (reaches down to 1μm) since the diameter of the taper decreases very fast when it etched to the size smaller than the initial core. And the loss due to tapering is not trivial.

Fabrication of the fiber taper by heating and pulling a SMF-28 optical fiber is much more successfully carried out. It combines the core and cladding into one rod in the tapered region, so that the evanescent wave can be effectively exposed. The heating source is pure hydrogen flame in air. The torch nozzle used for microsphere fabrication is changed to one with much smaller central drill (diameter<1mm), so that the flame can be adjusted to very small and concentrated on the fiber less than 5mm. Fig.4 shows the setup of fabrication. The middle of a fiber is stripped and cleaned for pulling. The fiber is then fixed by two fiber clamps (Thorlabs) on the pulling stage. One clamp is connected to a computerized programmable stepper motor (AMS), the other one is located on a 3-D differential translation stage (Thorlabs) which allows fine adjusting of the pulling alignment and post tensioning of the fiber taper. One end of the fiber is connected to a DFB 1531nm laser (NEL NLK1556STG) and the output signal is detected by a photodiode detector (Thorlabs). During the fabrication, the transmission signal is recorded and the hydrogen flame is brushed back and forth on the fiber. The stepper motor runs and accelerates for 16s until completed. A fiber taper of 1 to 2 in length inch is usually obtained with a waist that can disperses red, orange, yellow, green, blue and violet color light under white light. The dispersion indicates that the fiber taper diameter has reached to sub-micrometer scale. We did SEM measurement to confirm the size. Fig.5 shows that we have actually reached down to about 300nm of the taper waist. Fig.6 shows a typical transmission signal recorded during the fabrication which indicates that the power loss due to tapering is almost zero. The dense dips may be due to multimode interference when air becomes the cladding during the tapering. However, this needs to be confirmed in the future with further experimental study.

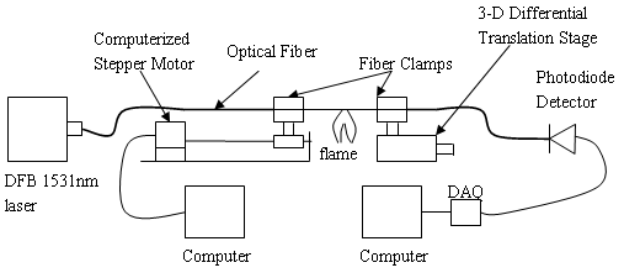

Fig.4 Setup of fiber taper fabrication by the method of heating and pulling.

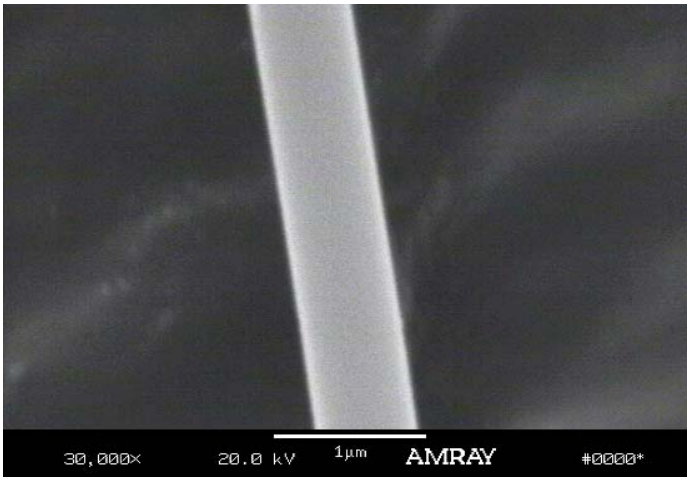

(a)

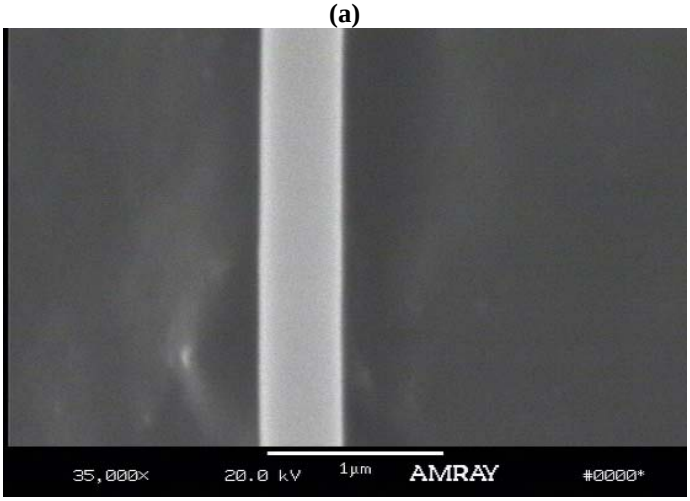

(b)

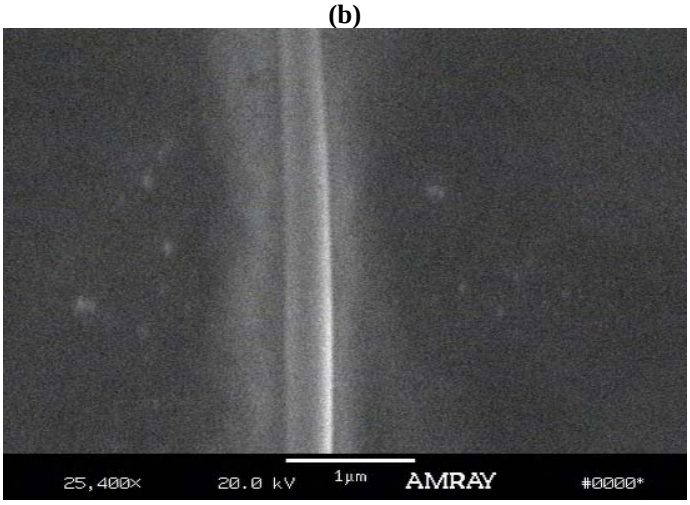

(c)

Fig.5 SEM image of the fiber waists of three different tapers.

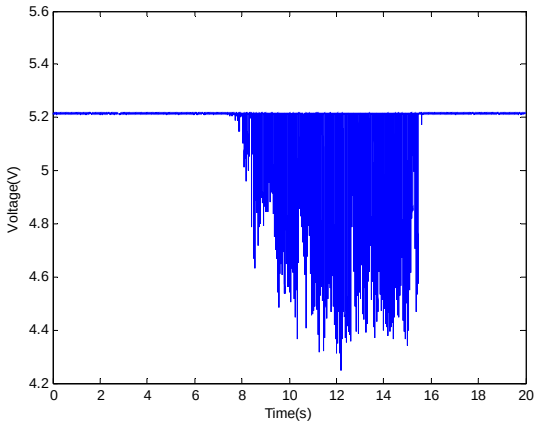

Fig.6 Monitoring transmission signal during fiber taper fabrication.

To preserve a fundamental mode light propagation in the tapered region, the adiabatic condition must be met. It assumes that all changes in fiber profile occur over such large distances that there is a negligible change in the power of local mode. We have the beat length[17]

$$z_b = 2\pi / \left|\beta_1 - \beta_2\right| \tag{1}$$

where β_1 and β_2 are the two closet propagation constants. Hence, the fiber nonuniformity must change over a distance large compared with z_b to ensure the fundamental mode propagation. For the single mode SMF-28 fiber, β_1 is the single mode propagation constant, while β_2 refers to a packet of radiation modes. And we can assume weakly guiding ($n_{co} \cong n_{cl}$) so that the upper bond of z_b can be expressed as[17]

$$z_b \cong \frac{4\pi a V}{(2\Delta)^{1/2}\tilde{W}^2} \tag{2}$$

where a is the radius of the core, $V = \frac{2\pi a}{\lambda}\left(n_{co}^2 - n_{cl}^2\right)^{1/2}$ is the waveguide parameter, $\Delta = \frac{1}{2}\left(1 - \frac{n_{cl}^2}{n_{co}^2}\right)$ is the profile height parameter and modal parameter $\tilde{W} \cong 1.123\exp(-2/V^2)$ for step refractive index profile fiber. Plugging in parameters of SMF-28 fiber, a=4.1μm, λ=1.531μm, n_{cl}=1.4647 and n_{co}=1.47, we have $z_b \cong 2.51mm$. For all the tapers we fabricated we have the transitional tapered region much longer than 2.51mm and thus have preserved the fundamental propagation.

4. WGM COUPLING OBSERVATION

Figure 7 shows a basic setup of WGM coupling. The DFB 1531nm tunable laser is tuned and launched into the fiber taper. The microsphere is positioned by a 3-D differential translation stage (Thorlabs) which has the finest step resolution of 20nm.

The coupling is manipulated under a microscope (Zeiss). The transmission signal is detected by a photodiode detector and recorded by a computer with DAQ.

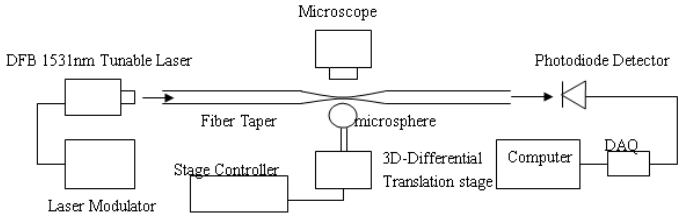

Fig.7 Setup of WGM coupling system

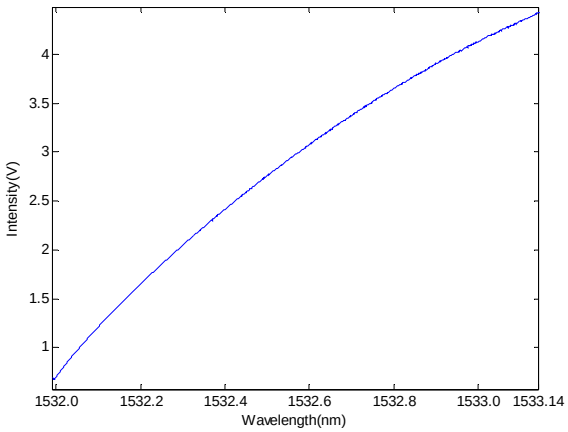

(a)

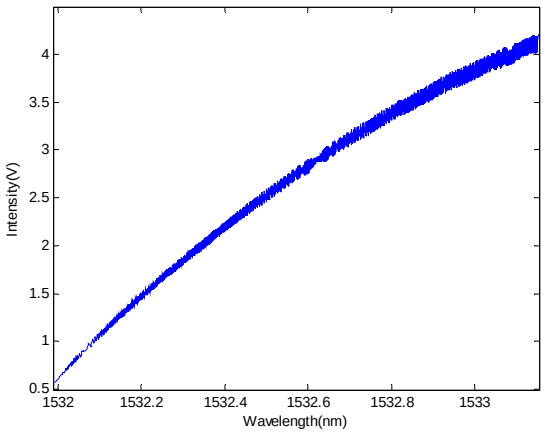

(b)

Fig.8 Transmission signal of ramp tuning (a) with angle cleaved output end and (b) without angle cleaved output end.

The output end of the fiber needs to be slightly angled cleaved to eliminate the etalon effect which results in significant oscillations on the ramp tuning curve. Fig.8 shows the etalon effect by comparing differently cleaved fiber output end.

The WGM is characterized by three mode numbers *n*, *l*, and *m* which are the radial, angular, and azimuthal mode numbers, respectively. We are interested to excite fundamental modes with low *n* and with $m \approx l$, which are the modes with smallest mode volume and most closely confined to the surface of the sphere and to the sphere equator ($|m|=l$). To get an efficient excitation of these WGM's, sizes of the fiber taper and microsphere must be chosen by matching the propagation constants of these two coupling components. According to the calculation by J. C. Knight et al.[12], a sphere with a diameter about $50\mu m$ matches to a taper waist with diameter about $2.8\mu m$, and a sphere with a diameter about $500\mu m$ matches to

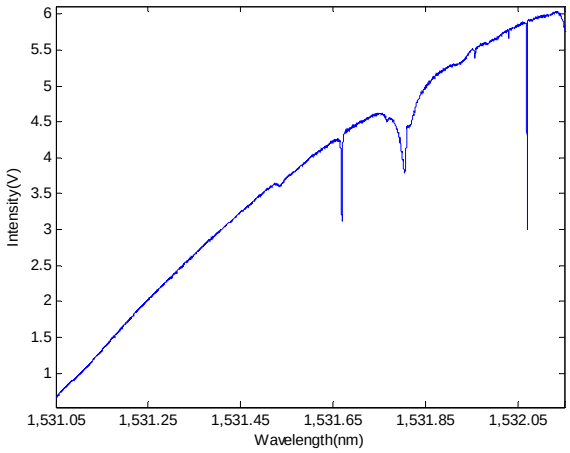

Fig.9 WGM spectrum of a microsphere with D=58μm coupled with taper waist where locally diperses blue light.

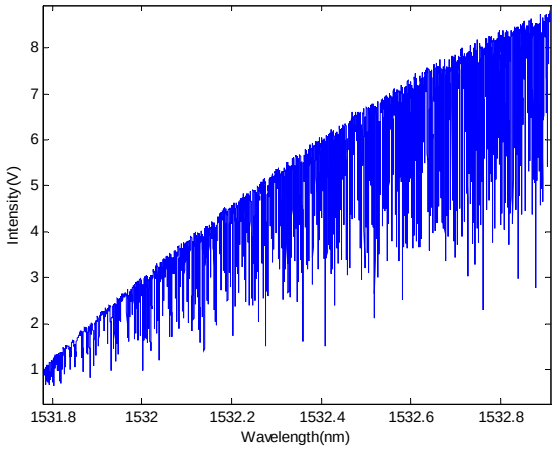

Fig.10 WGM spectrum of a microsphere with D=490μm coupled with taper waist where locally diperses green light.

a taper waist about $5\mu m$. These two sphere sizes are the two limits of our fabrication capability of melting a single fiber or fiber taper. By directly touching the equator of the sphere to different parts of the fiber taper waist, different transmission coupling spectrums can be observed. Fig.9 shows the spectrum of a microsphere with diameter about $58\mu m$ coupled to a taper waist where locally disperses blue light (which means sub-micron diameter). The wavelength tuning range is about

1.11*nm*, which is measured by an optical spectrum analyzer (ANDO). This coupling has been optimized to obtain the smallest mode volume. We can see that taper waist is much smaller than the theoretical prediction for phase matching. Fig.10 shows a coupling with a mismatch of the propagation constants. The wavelength tuning range is about 1.13*nm*. It is a microsphere with diameter about 490μm coupled with the taper waist that locally disperses green light. A large number of WGM have been excited. Fig.11 is another optimized to smallest mode volume coupling, with sphere size D=225μm and taper that does not disperses visible light (which indicate diameter is more than 1μm). The wavelength tuning range is about 1.27*nm*. Since we have the similar wavelength scan ranges among the three cases, it is demonstrated that the smaller the sphere the less WGM that can be excited.

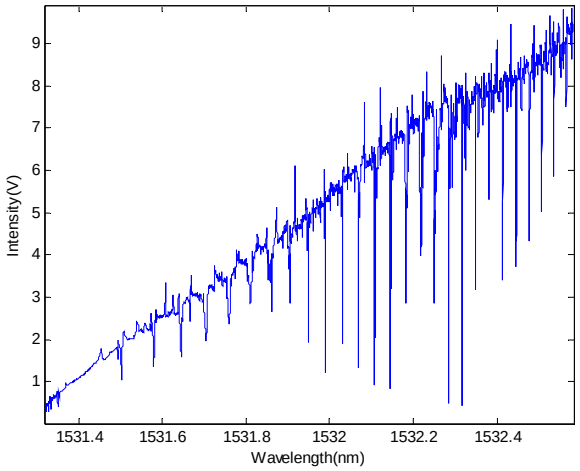

Fig.11 WGM spectrum of a microsphere with D=225μm coupled with taper waist that locally does not disperses visible light.

Q value is another important quality that characterizes a resonator. It is defined as [18]

$$Q_T = \frac{f_0 E}{P} \tag{3}$$

where Q_T is the total *Q* value of the WGM, f_0 is the WGM resonance frequency, *E* is the energy stored in a fully charged WGM and *P* is the loss rate of the stored energy. A simpler formula for calculating *Q* can be deduced as [18]

$$Q_T = \frac{f_0}{\Delta f} \tag{4}$$

where Δf is the linewidth of the WGM. So by measuring Δf, we can calculate the *Q* value. Apparently the sharper the dips on the transmission spectrum like the ones shown in Figs.9~11, the higher the *Q* value. However, the laser's bandwith is finite and thus the linewidth of the dip (WGM) results from a convolution effect of the laser's and WGM's lineshapes. Assume both lineshapes are Lorentzian, Δf can be deduced as

$$\Delta f = FWHM_1 - FWHM_2 \tag{5}$$

where $FWHM_1$ is the WGM dip's full width at half maximum measured in experiment, and $FWHM_2$ is essentially the bandwidth of the laser. Using (4) and (5), the total *Q* value of sharpest dip in Fig.9 is determined as about 3.2×10^6, which is for a sphere with diameter about 58μm. And total *Q* value of a sphere with diameter about 490μm can easily achieve 4×10^7. The total *Q* value can also be expressed as [9]

$$\frac{1}{Q_T} = \frac{1}{Q_m} + \frac{1}{Q_s} + \frac{1}{Q_c} + \frac{1}{Q_r} + \frac{1}{Q_{cp}} \tag{6}$$

Where Q_m, Q_s, Q_c, and Q_r account for material loss, scattering loss, loss due to surface contamination, and radiation loss due boundary curvature respectively. And they give the intrinsic *Q* value Q_{in}. Q_{cp} accounts for the coupling loss. Q_{cp} increases as sphere detaches from the taper and moves away from the taper. At certain distance of the sphere to the taper, $Q_{in}=Q_{cp}$ which is usually defined as critical coupling[19]. And the total *Q* value is half of the intrinsic *Q* value at this point. The couplings are defined as overcoupling and undercoupling when this distance decreases and increases respectively. And the total *Q* value is less than half and more than half of the intrinsic *Q* value respectively. Thus Q_{in} of the 490μm sphere is believed to have achieved to 10^8.

By post tensioning the fiber taper and putting an electric-static charge eliminator (Staticmaster) in proximity of the coupling system, the effect of the fiber taper jumping onto the sphere can be efficiently reduced. With the 20*nm* step resolution differential translation stage, spaces between the taper and sphere can be leaved for achieving the three kinds of couplings. The coupling efficiency is represented by introducing a coupling coefficient which is defined as the ratio of WGM dip amplitude over the signal intensity where the corresponding dip begins. Fig.12 shows a WGM's coupling coefficient varying with the distance between the sphere and fiber taper. The three different coupling regimes can be clearly distinguished in the graph. Point c is approximately the critical coupling point, where most of the transmission power is coupled into the microsphere. And on the right and left of point c is undercoupling and overcoupling regimes respectively. The sphere diameter is about 80μm. By scanning the laser with a range about 0.016*nm*, we get Fig.13 in which (a) to (f) correspond to the coupling points a, b, c, d, and f marked in Fig.11. The linewidth of WGM increases a lot from (a) to (f). For this special case, the total *Q* value decreases from 1.5×10^7 down to 1.5×10^5. Thus leaving a space is crucial for increasing *Q* value and varying the coupling coefficient.

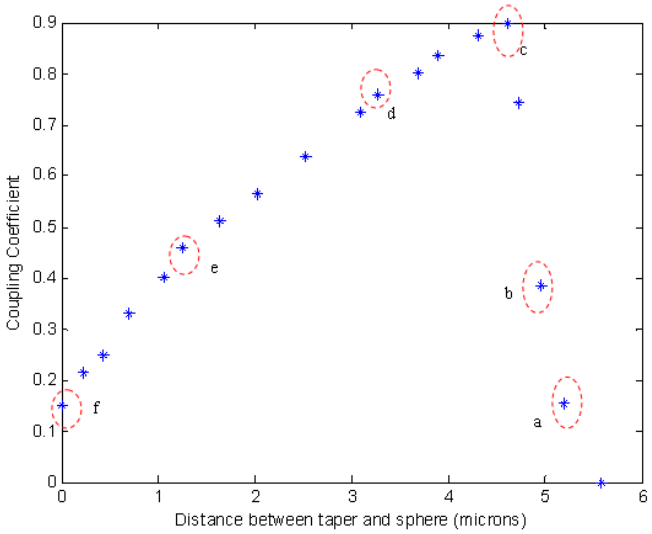

Fig.12 Coupling coefficients of a WGM for the sphere at different distances from the fiber taper (sphere diameter=80 *μm*).

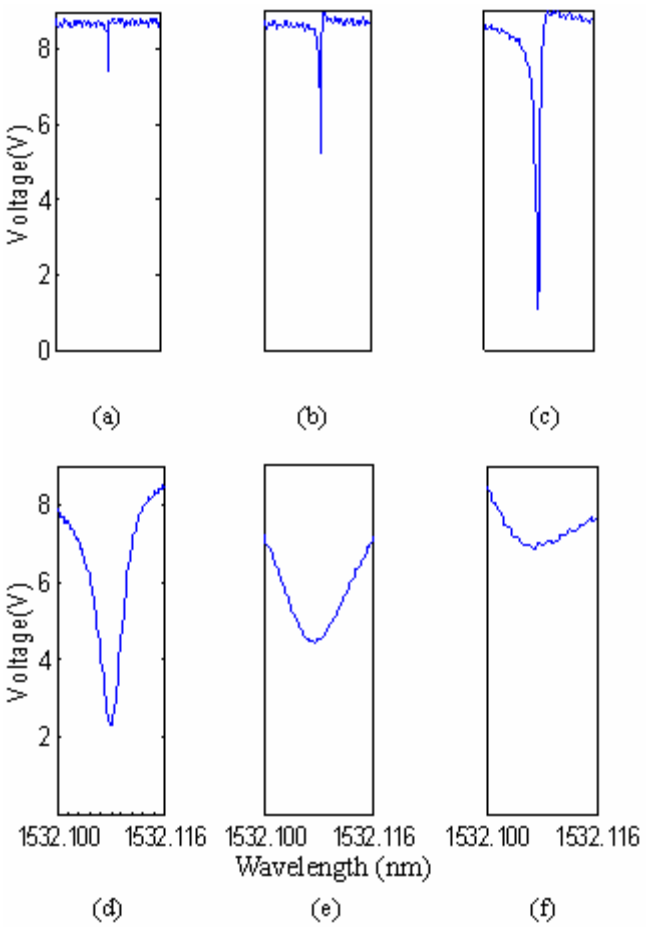

Fig.13 A WGM in different coupling regimes (sphere diameter=80*μm* wavelength scan range=0.016*nm*).

5. SENSOR APPLICATIONS OF WGM

5.1 Temperature Sensing by WGM shift

The resonance frequency of a WGM shifts when the effective refractive index and diameter of the microsphere changes. A novel temperature sensor can be built based on this mechanism. Assume that the WGMs are concentrated on the circumference of the equatorial plane of the sphere, which are the fundamental modes. Assume there are *m* EM field maxima on the circumference which is much longer than the resonance wavelength, we have

$$\pi D = m\frac{\lambda}{n} \tag{7}$$

where D and *n* are the microsphere's diameter and refractive index respectively, λ is the resonance wavelength. Thus,

$$\frac{dn}{n}+\frac{dD}{D}=\frac{d\lambda}{\lambda} \tag{8}$$

We also have

$$\frac{dD}{D}=\alpha dT \quad \text{and} \quad \frac{dn}{n}=\beta dT \tag{9}$$

where $\alpha = 0.55\times10^{-6}/K$ [20] which is the linear coefficient of thermal expansion of fused silica, and its thermo-optic coefficient $\beta = 8.57\times10^{-6}/K$ [21].

Plugging (9) into (8) gives

$$(\alpha+\beta)\lambda=\frac{d\lambda}{dT}\ . \tag{10}$$

Plugging in the constants and using $\lambda = 1531nm$ (the wavelength of the scanning laser) we have

$$\frac{d\lambda}{dT}\approx 0.014nm/K\ . \tag{11}$$

We use this to sense air's temperature change around the microsphere. For the experimental setup, we simply attach a copper plate on a temperature controllable digital hot plate (CIMAREC) with high conductive silicone paste. The hot plate is located on a two dimensional translational stage so that the copper plate can be moved below and close to the coupling system. The temperature of the heat plume of the copper plate will alter the air temperature around the resonator. A thermalcouple is positioned less than 1mm close to the coupling system by another 3-D translational stage in order to approximately measure the temperature sensed by the WGM coupling system. The wavelength is scanned at 100*Hz* with a range of 1.128*nm*, and the WGM shift is counted from the beginning of each scan. The spectrum is recorded at different temperatures read by the thermal couple. Fig.14 shows the sensing result of a sphere with D=47*μm*. Every WGM shift is recorded when the temperature read from the thermalcouple is stabilized for at least 2s. The sensitivity is about 0.017*nm*/*K* which is very close to the theoretical prediction of 0.014*nm*/*K*.

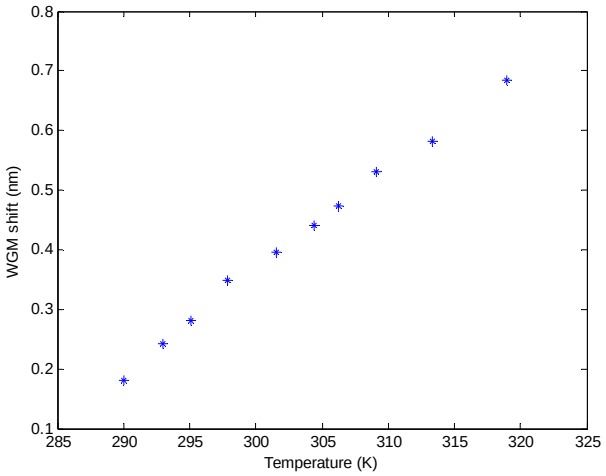

Fig.14 Temperature sensing curve vs. the WGM shift

Next, we analyze the sphere's temperature response. For the case of fluid flowing across a sphere, we can use[22]

$$Nu = 2 + \Pr^{0.4}(0.4\,\mathrm{Re}^{0.5} + 0.06\,\mathrm{Re}^{2/3}) \tag{12}$$

For rough but reasonable estimate, assume the speed of the flow across the sphere is 0.5m/s, and plug in air's properties at 25 ^{o}C. We have $\mathrm{Re} \approx 1.52$, $\Pr \approx 0.702$ and thus $Nu \approx 2.5$.

$$h = Nu \cdot k / D \tag{13}$$

Using air's conductivity coefficient $k = 0.029W/(m \cdot K)$

We have $h = 1542W/K$, and $k_{SiO2} = 1.38W/(m \cdot K)$. Thus

$$Bi = \frac{hD}{k_{SiO2}} = 0.053 < 0.1 \tag{14}$$

And obviously the *Bi* number is even smaller if the flow speed is less than 0.5*m/s* as estimated. Therefore, lumped analysis method for sphere is valid. In other words, the sphere's temperature can be assumed to be uniformly changed in the experiment. The time constant of the temperature response of the sphere is

$$\tau = \frac{\rho c V}{hA} = 0.008s \tag{15}$$

where silica density ρ=2.2×10^3*kg/m*^{3} and specific heat *c*=703*J/(kg.K)* [20]. This proves that the temperature sensing of the WGM has a fast response which is superior to a typical thermalcouple which may have a response time from 0.1s to seconds.

5.2 Trace gas sensing by Cavity Ring Down

Cavity Ring Down(CRD) spectroscopy is a form of laser absorption spectrometry. Usually, a laser pulse is trapped in a detection cavity built with two highly reflective mirrors. The intensity of the trapped pulse will decrease by a fixed percentage during each round trip within the cavity due to both absorption by the medium within the cavity and reflectivity losses. Because of the long absorption path that light bounce around in the cavity, CRD spectroscopy always has much higher sensitivity than traditional spectroscopy. We propose an idea of using the WGM to do CRD spectroscopy, which may complete the long path absorption and maintain a high sensitivity in a much smaller volume than a traditional one. As a WGM is fully charged (the transmission signal goes down to the bottom of dip), the laser can be instantly blocked. Then the transmission signal should be fully due to the light coupling back from the sphere into the fiber taper. The power of the evanescent wave around the sphere due to light propagation inside can be absorbed by the surrounding medium. Thus, the decay time of the light leaking out into the fiber taper, or in other words, the life time of photon inside the microsphere will be shortened. By detecting the decaying transmission signal in the output end of the fiber taper, the medium around the microsphere can be detected. The photon's 1/e life time in the microsphere can be estimated as [23]

$$\tau = \frac{Q}{2\pi f_0} \tag{16}$$

If the *Q* value is above 10^8, for a WGM resonance around 1531*nm*, i.e. f_0=1.96×10^{14}*Hz*, we will have τ≅81*ns* which corresponds to a path more than 25*m*.

We choose ammonia as a designed species around the microsphere for absorption, since it has a dense absorption lines around the telecommunication wavelength 1550*nm*. We use the linestrengths from Lundsberg-Nielsen[24]. To demonstrate this sensor, we specifically choose an absorption line of NH_3 at v_0=6529.185cm^{-1}(1531.585*nm* where our tunable DFB 1531*nm* laser can cover), which has a typical magnitude of linestrength around 1531*nm*. The line profile can be simulated as Fig.15. Suppose we have one WGM park at v=6529.165cm^{-1}(1531.589*nm*), the related absorption linestrength is indicated in Fig.15 by the doted line. If the pressure of the pure NH_3 is 9.8torr and temperature is 21^{o}C, the absorbance will be 1.0987×10^{-3}cm^{-1} calculated from the linestrength. And for cavity ring down spectroscopy, we have[25]

$$K\nu = \frac{1}{c}\left(\frac{1}{\tau_1} - \frac{1}{\tau_2}\right) \tag{17}$$

Where τ_1 is the time constant of cavity ring down with NH_3 around the microsphere and τ_2 is the one with absence of NH_3. If the *Q* factor is 10^8 initially without NH_3, τ_2 is then 81ns as estimated by Eq.(16) and τ_1 will be 22*ns* according to Eq.(17). 59*ns* time constant change can be achieved. Thus, we have shown the possibility of building such a sensor for trace gas.

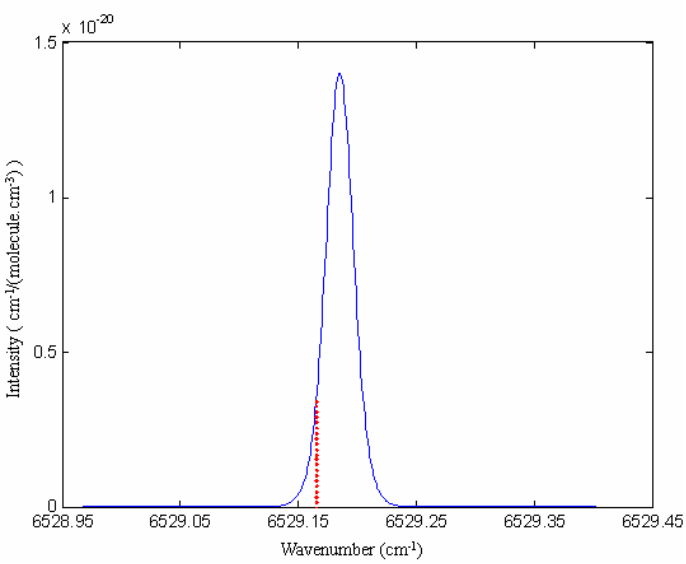

Fig.15 Absorption line of NH3 at v_0=6529.185cm^{-1}.

6. CONCLUSION

To summarize, we have used a strict method to clean SMF-28 stripped fiber and fabricated microspheres with sizes ranging from about 50μm to about 500μm. Fiber tapers with sub-micron waist sizes are fabricated by heating and pulling stripped fiber of the same material. It is observed that the tapering loss is negligible for these fiber tapers. Various WGM coupling spectra are recorded for coupling systems of different sizes of the sphere and fiber taper. By eliminating the influence of electrostatic charge, an effective gap (0-5μm) between fiber taper and microsphere is made and different regimes of coupling are achieved. *Q* value and coupling efficiency can be flexibly controlled over the different coupling regimes. *Q* value could vary from 1.5×10^7 to 1.5×10^5 for the special case we measured. A temperature sensor for air is demonstrated using WGM shifts. Its sensitivity (0.017*nm/K*) from the experimentql measurement agrees very well with the one (0.014*nm/ K*) predicted by theory. The concept of using WGM as cavity ring down spectroscopy is proposed. The calculation shows that ammonia at room temperature with low pressure of 9.8 torr could cause a cavity ring down time constant change of 59 *ns*.

ACKNOWLEDGEMENTS

T. Rossmann and Z. Guo are grateful for the support of an Academic Excellence Funds Award from Rutgers University. Part of this material is also based upon work supported by the National Science Foundation under Grant No. CBET-0651737.

REFERENCES

[1] D.W. Vernooy, A. Furusawa, N.P. Georgiades, V.S. Ilchenko, H.J. Kimble, Phys. Rev. A 57 (1998) R2293.

[2] V.V. Vassiliev, V.L. Velichansky, V.S. Ilchenko, M.L. Gorodetsky, L. Hollberg, A.V. Yarovitsky, Opt. Commun. 158 (1998) 182.

[3] V. Sandoghdar, F. Treussart, J. Hare, V. Lefe`vre-Seguin, J.-M. Raimond, S. Haroche, Phys. Rev. A 54 (1996) 1777.

[4] M. Cai, O. Painter, K.J. Vahala, P.C. Sercel, Opt. Lett. 25 (2000) 1430.

[5] F. Lissillour, P. Fe′ ron, N. Dubreuil, P. Dupriez, M. Poulain, G.M. Ste′ phan, Electron. Lett. 36 (2000) 1382.

[6] S.I. Shopova, G. Farca, A.T. Rosenberger, W.M.S. Wickramanayake, N.A. Kotov, Appl. Phys. Lett. 85 (2004) 6101.

[7] H. Quan and Z. Guo, "Simulation of whispering-gallery-mode resonance shifts for optical miniature biosensors," J. Quantitative Spectroscopy & Radiative Transfer 93 (2005), pp: 231-243.

[8] I. Teraoka, S. Arnold, and F. Vollmer, "Perturbation approach to resonance shifts of whispering-gallery modes in a dielectric microsphere as a probe of a surrounding medium," J. Opt. Soc. Am. B 20, 1937-1946 (2003).

[9] M. L. Gorodetsky, A. A. Savchenkov, and V. S. Ilchenko， "Ultimate Q of optical microsphere resonators," OPTICS LETTERS April 1, 1996 / Vol. 21, No. 7

[10] J. Stratton et al., "Elliptic cylinder and spheroidal wave functions including tables of separation constants and coefficients", Wiley, New York, 1941.

[11] J. C. Knight, N. Dubreuil, V. Sandoghdar, J. Hare, V. Lef`evre-Seguin, J. M. Raimond, and S. Haroche, "Mapping whispering-gallery modes in microspheres with a near-field probe," OPTICS LETTERS, July 15, 1995 / Vol. 20, No. 14

[12] J. C. Knight, G. Cheung, F. Jacques, and T. A. Birks, "Phase-matched excitation of whispering-gallery-mode resonances by a fiber taper," OPTICS LETTERS, August 1, 1997 / Vol. 22, No. 15

[13]Collot L., Lefevreseguin V., Brune M., Raimond J. M., and Haroche S., "Very High-Q Whispering-Gallery Mode Resonances Observed On Fused-Silica Microspheres." Europhysics Letters, 1993. 23(5): p. 327-334.

[14]Ilchenko V. S., Yao X. S., and Maleki L., "Pigtailing the high-Q microsphere cavity: a simple fiber coupler for optical whispering-gallery modes," Optics Letters, 1999. 24(11): p. 723-725.

[15] J.-P. Laine, B.E. Little, D.R. Lim, H.C. Tapalian, L.C. Kimerling and H.A. Haus, "Microsphere resonator mode characterization by pedestal anti-resonant reflecting waveguide coupler," IEEE Photonics Technol. Lett. **12** (2000), pp. 1004–1006.

[16] Adiabatic Flame Temperature. The Engineering Toolbox. http://www.engineeringtoolbox.com/adiabatic-flame-temperature-d_996.html

[17] A. W. Synder and J. D. Love, "Optical Waveguide Theory," Chapman & Hall, London, 1983

[18] Christopher C. Davis, "Lasers and Electro-Optics: Fundamentals and Engineering," Cambridge University Press 1996.

[19] Ming-Chang M. Lee, Ming C. Wu, “Tunable coupling regimes of silicon microdisk resonators using MEMS actuators,” OPTICS EXPRESS, 29 May 2006 / Vol. 14, No. 11

[20] http://accuratus.com/fused.html

[21]Douglas B. Leviton and Bradley J. Frey, “Temperature-dependent absolute refractive index measurements of synthetic fused silica” Proc. of SPIE Vol. 6273, 62732K, (2006)

[22] INCROPERA Frank P, DEWITT David P., “Fundamentals of heat and mass transfer,” 1996 - John Wiley & Sons, New York

[23] Fan X., Doran, A. and Wang, H., “High-Q Whispering Gallery Modes from a Composite System of GaAs Quantum Well and Fused Silica Microsphere,” Applied Physics Letters, Vol. 73, No.22, pp. 3190-3192

[24] L. Lundsberg-Nielsen, F. Hegelund, and F. M. Nicolaisen, “Analysis of the High-Resolution Spectrum of Ammonia ($^{14}NH_3$) in the Near-Infrared Region, 6400~6900cm^{-1},” Journal of Molecular Spectroscopy, 162:230-245, 1993

[25] Kenneth W. Busch, Marianna A. Busch, “Cavity-Ringdown Spectroscopy: An Ultratrace-Absorption Measurement Technique,” 1999 American Chemical Society, Oxford University Press